

Synthesis, Characterization and Application of Zinc Oxide Nanoparticles for Textile Materials against Ultra Violet Radiation

Bulcha Bekele^{1*}, Gemechu Berhanu² and Desalegn Shiferaw³

¹Dambi Dollo University, College of Natural and Computational Science, Department of Physics.

²Dambi Dollo University, College of Veterinary Agriculture and Medicine

³Dambi Dollo University, College of medicine and Healthy Science, Department of Public Health.

Abstract:- Nanoparticles are a part of nanotechnology with the dimension of 1nm-100m. The aim of this paper is to synthesis, characterizations, compares the treated and untreated cotton textiles. Zinc oxide nanoparticles (ZnONPs) were synthesized by sol-gel method from zinc acetate dehydrate ($Zn(CH_3COO)_{2.2}H_2O$), zinc sulphate heptahydrate ($ZnSO_4 \cdot 7H_2O$) and zinc nitrate hexahydrate $Zn(NO_3)_2 \cdot 6H_2O$ as a precursor with sodium hydroxide and polyvinyl alcohol concentration at the same annealing temperature of 400°C. The synthesized ZnONPs were characterized by X-Ray Diffraction (XRD), Scanning Electron Microscopy (SEM) and UV/vis spectroscopy. The X-RD results, revealed that the synthesized nanoparticles has wurtzite hexagonal structure with the average particle size of 44±50nm, 42±30nm, 30±32nm from zinc nitrate hexahydrate and polyvinyl alcohol concentration (S1), zinc acetate and sodium hydroxide (S2), zinc sulphate heptahydrate and sodium hydroxide (S3) samples respectively. The SEM images of synthesized ZnONPs using S1 sample was flower in shape and spherical for S2 and S3. The results, obtained from SEM are agreed with that of XRD. The UV/vis absorption peaks were observed at 350nm and 390nm using S1, 378nm and 380nm using S2 and S3 and exhibits 3.536eV, 3.274eV, and 3.257eV energy band gap using S1, S2, and S3 respectively. The energy band-gap of ZnONPs was blue-shifted by the effect of quantum confinement when compared with bulk ZnO. The peaks observed from UV/vis absorption were due to electronic transition from valiancy band to conduction band. The synthesized ZnONPs were applied on cotton textiles to impart sunscreen activity of treated cotton textiles. The effectiveness of treatment was assessed using UV/vis spectroscopy. The ultraviolet protection factors (UPF) and percent of transmissions (%T) found to be good ultraviolet radiation blockers. Treated cotton textiles reduce the harm full impacts of UV radiations on human skin.

Keywords:- Characterization; Synthesis; Textiles; UV-Radian; ZnONPs.

I. INTRODUCTION

Nanotechnology is the technology that deals with synthesis, characterizations, exploitations and exploration of nanoparticles with structural features between their bulk and their nanomaterials. In other word, it is the technology of design and application of nanoparticles with fundamental properties and functions [1]. Nanoparticles are also the part of nanomaterials with dimension of 1nm to 100nm and had great advantages in modern technology of textile industries. In addition, nanoparticles had great applicable in life science, medical, biomedical, healthy care, and security, agriculture, production of energy, store energy, energy conservation, infrastructure, building and constructions [2].

Among several nanoparticles, ZnONPs have shown a great importance in many applications due to its capability of absorbing light, transport charges, and provide fast response, low cost and easy to use. Several literatures reported that, zinc oxide nanoparticles applicable to textiles materials in UV-blocking properties, anti bacterial activities, ant fungal, self cleaning, sun screening, food packaging, water and air purification, sterilizing environment, biomedical, cosmetics, photo-catalyst due to its unique physical and chemical properties i.e. high chemical stability, high electro chemical coupling coefficient, broad range of radiation absorptions, wide energy band gap(3.37eV), large exciton binding energy(60meV), high thermal and mechanical stability[3-4]. ZnONPs shows excellent properties such as easy to synthesis, non-toxic, controlled shape and size, presence of intrinsic and extrinsic at emission center, emitting different colors (violet, blue, green, yellow, and red) [5].

Due to green house effect, the protections of ultraviolet radiation are one of the most important concerns in textiles industries. Ultraviolet radiation is a form of energy that comes from sunlight having 50% visible light, 45% infrared and 5% ultraviolet radiations [6]. According to its wavelength effect, ultraviolet radiation can be categorized into ultraviolet (UVA) (400nm-320nm), ultraviolet UVB (320nm-280nm), and ultraviolet (UVC) (280nm-200nm) and from these, UVC is

does not reach the earth's surface due ozone layer. UVA and UVB are the most dangerous radiation having shorter wave length with higher energy [7]. Several research are done on textiles to block the effects of UV-radiation by synthesizing nanoparticles and the synthesized nanoparticles have three main structure including cubic rock salt, Hexagonal and cubic zinc blende structures in which hexagonal structures is thermodynamically stable under ambient conditions[8]. Nano-flower, nano-wire, nano-belts, nano-combs, nano-springs, nano-cages, needle-like, nano-ring, nano-helix, nano-flake, spherical, bullet-like, sheet, polyhedral, hexagonal plate, nano-rod, nano tube, pyramid shape, malty sphere, dough-nut like, nano-leafs, nano-bows and star, multi-pods and spike, cylinder like, crushed stone like, ellipsoid are some shapes of zinc oxide nanoparticles obtained from scanning electron microscope[5-9]. Excellent ultraviolet blocking properties of ZnONPs are related to absorbance of UV-radiation through semi-conductive whether they are highly refractive/scattering radiations. Moreover, the protective mechanisms of ZnONPs are directly depends on the chemical structure of the particles. In addition, it also depends on particle size, shapes, crystalline and crystal form [7-10]. Absorption, direct transmission, and scattering are observed when textiles materials exposed to ultraviolet radiation. The transmitted ultraviolet radiation causes skin damage, fiber dye. Reflection and absorbance UV-radiations are expressed interns of ultraviolet protective factors (UPF) is a measure of blocking UV-radiations by textiles. The higher UPF value the more protective [11].

A variety of preparation techniques have been reported for the synthesis of ZnONPs includes sol-gel [12], hydrothermal [13], spray-pyrolysis [14], electro-spinning [15], Photo-chemical [16] methods. In our case, sol-gel methods were used to synthesis ZnONPs from zinc acetate dehydrate ($Zn(CH_3COO)_2 \cdot 2H_2O$), zinc sulphate heptahydrate ($ZnSO_4 \cdot 7H_2O$) and zinc nitrate hexahydrate ($Zn(NO_3)_2 \cdot 6H_2O$) precursors with sodium hydroxide and polyvinyl alcohol concentration of the same annealing temperature. The XRD result show that, the exsitu-synthesized nanoparticles [17], have an average size of 39nm, were coated onto bleached cotton fabrics. In addition, the synthesized nanoparticles are characterized by scanning electron microscope, UV/vis spectroscopy of treated and untreated cotton textiles. Therefore, the aim of this research is to synthesis, characterization, compare and contrast the treated and untreated cotton textiles.

II. MATERIALS AND METHODS

2.1 Materials

The chemical used in this work were zinc nitrate hexahydrate ($Zn(NO_3)_2 \cdot 6H_2O$), Zinc acetate dehydrate ($Zn(CH_3COO)_2 \cdot 2H_2O$), zinc sulphite heptahydrate ($ZnSO_4 \cdot 7H_2O$), Sodium hydroxide (NaOH), and Polyvinyl Alcohol ($[-CH_2CHOH-]_n$) are purchased from Himedia, India: assay>99.2%.

2.2 Synthesis Methods

ZnONPs were synthesized by sol-gel method [19]. Here, ZnONPs were synthesized from polyvinyl alcohol ($[-CH_2CHOH-]_n$) and zinc nitrate hexahydrate ($Zn(NO_3)_2 \cdot 6H_2O$), Sodium hydroxide (NaOH) and zinc acetate dehydrate ($Zn(CH_3COO)_2 \cdot 2H_2O$), and sodium hydroxide (NaOH) and zinc sulphite heptahydrate ($ZnSO_4 \cdot 7H_2O$) as follow. All the glass beakers were first cleaned and rinsed with distilled water and dried in dry oven. Then after, 6gm of polyvinyl alcohol and 2gm of zinc nitrate hex-hydrate($Zn(NO_3)_2 \cdot 6H_2O$) were weighted by beam balance and dissolved into 60ml and 20ml of double distilled water respectively. Then, it was stirred continuously with gentle magnetic stirrer until its temperature is raised to 90°C. While the temperature of polyvinyl alcohol solution was reached 90°C, 0.34M of zinc nitrate hex-hydrate solution was added drop by drop without touching the wall of container. Then, the aqueous solutions were turned into a milky white colloid without any precipitation. After this, the reaction were allowed to proceed for two hours after complete the addition of zinc nitrate hexahydrate. After the reaction is completed, the solution was allowed to settle and the supernatant solution was removed by washing with double distilled water three times. After washing, the precipitate is allowed to dry in oven at 150°C for 12hr. Next to this, the samples from oven were taken into furnace (Model no: MC2-5/5/10-12, Biobase, China) by crucible and calcinated for 8hr at 400°C. By similar procedure, ZnONPs were synthesized from NaOH and zinc acetate dehydrate ($Zn(CH_3COO)_2 \cdot 2H_2O$), zinc sulphite heptahydrate ($ZnSO_4 \cdot 7H_2O$) were NaOH used as Chelating agent for these two precursors.

2.3 Characterization Methods

X-Ray Diffraction (XRD) pattern of ZnO nanoparticles were obtained using XPERT-PROX-Ray Diffractometer generating $Cu-K_{\alpha}$ radiation ($\lambda=1.5418\text{\AA}$). It is used to determine the crystalline size of the synthesized nanoparticles. Small amount of powder sample were used for characterization. X-ray generators were operating at a voltage of 40kV and apply a current of 30mA at room temperature. Intensities were measured at room temperature in steps of 0.02, over the range of $10^0 < 2\theta < 80^0$, and the Diffractometer is connected to a computer for data collection and characterization displays. The peaks of the X-ray diffraction pattern were compared with the standard available data for the confirmation of the structure.

About, 0.6g of synthesized ZnONPs was grinded to fine powders and measured by beam balance, and taken to metal plate. Then, the morphology of the resulting nanoparticles were studied by using scanning electron microscope (Hitachi, H-7600), which is operates under high vacuum and has

magnification ranging from 20X to approximately 30,000X, spatial resolution of 50 to 100 nm. The fixed sizes, higher magnification of ZnONPs were obtained by reducing the raster size of the specimen, and vice versa.

Absorbance spectra of ZnONPs were measured using UV/vis Spectroscopy (Perkin Elmer, Lambda 950), by using 1 cm quartz cuvette over 200-500nm range of wavelength. About 0.3gm of ZnONPs was dissolved in double distilled water and their solutions were poured into quartz cuvette. Then, the cuvette is taken in to Ultraviolet Visible Spectrophotometer and the absorbance spectra of ZnONPs were measured. White cotton fabrics, was purchased from Local, Oromia Regional State of Ethiopia. The samples (10 cm x 10 cm) with mass per unit surface of 50g/m² for cotton were prepared. In order to remove unnecessary particles from the fabric sample it was washed five times using distilled water and ethanol alcohol. The fiber was soaked in a solution of ZnONPs, for 10min under gentle magnetic stirring. The cloth was then squeezed to remove the excess dispersion and dry in oven at 130°C for 15min. The effectiveness in shielding UV-radiation was evaluated by measuring the UV-absorption, and transmission.

III. RESULTS AND DISCUSSION

3.1 X-RD Analysis of ZnONPs

Figure 4.1 shows intensity versus angle of diffraction of X-ray diffraction spectra of zinc oxide nanoparticles prepared by chemical precipitation methods of Polyvinyl alcohol(PVA) and Zinc nitrate hexahydrate Zn(NO₃)₂.6H₂O, Sodium hydroxide (NaOH) and Zinc acetate (Zn(CH₃COO)₂.2H₂O), zinc sulphite heptahydrate(ZnSO₄.7H₂O) and (NaOH) which is represented by sample S1, S2, and S3 respectively. The spectra shows well defined peaks of ZnONPs. About nine characteristic peaks were observed at 31.74°, 34.40°, 36.23°, 47.60°, 56.59°, 62.87°, 66.39°, 67.97° 69.10° and their corresponding reflection from (100), (002), (101), (102), (110), (103), (200), (112), (201), respectively for these three samples. The samples peak (101) is the most intense peak and the broad diffraction peaks without peak shift. The presence of several peaks indicates that the random orientation of the crystallites. The full width at half maxima of synthesized nanoparticles is almost the same for these of three samples.

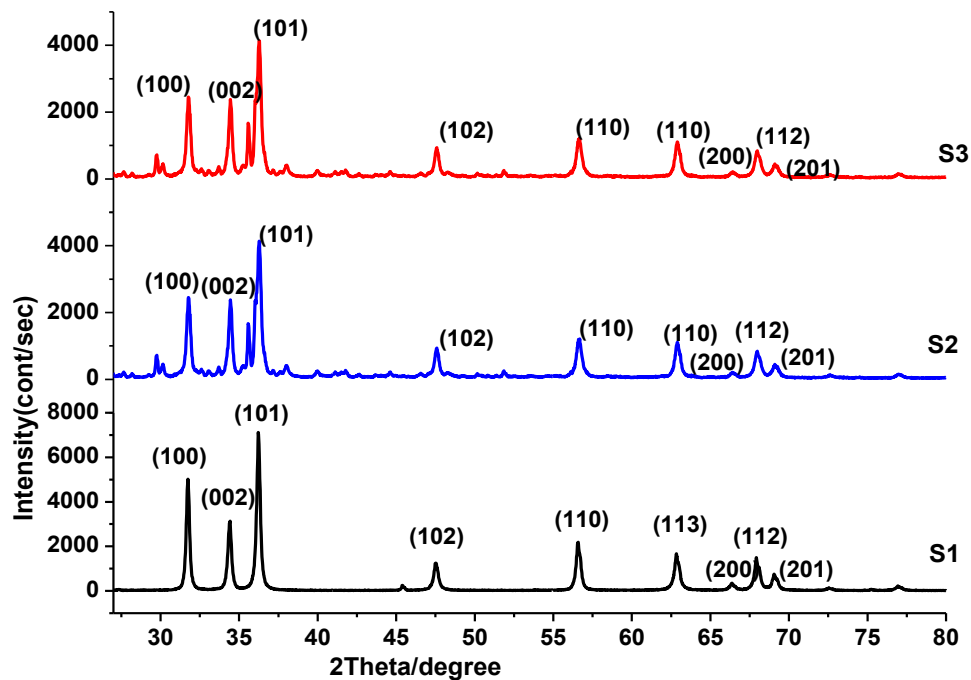


Figure 4.1. XRD diffraction pattern of synthesized ZnONPs of sample S1, S2 and S3.

The average particle sizes (D) of synthesized ZnONPs using samples S1, S2 and S3 were calculated by Debye- Scherrer equation of (4.1).

$$D = \frac{0.89 \lambda}{\beta \cos \theta} \quad (4.1)$$

Where, λ is wavelength of X-Ray diffraction ($\lambda = 0.154$ nm), β is FWHM (Full Width at Half Maximum) in radians, θ is the diffraction angle and D is particle size [20]. The average particle sizes of synthesized ZnONPs using samples S1, S2 and S3 were 44 ± 50 nm, 42 ± 30 nm, and 30 ± 32 nm respectively and recorded into table 4.1.

Table 4.1. Angle of diffraction, full width at half maxima and average particle size of synthesized ZnONPs using S1, S2 and S3

S1							
No.	$\theta(^{\circ})$	$2\theta(^{\circ})$	Hkl	FWHM	Size	D(nm)	Standard $2\theta(^{\circ})$ JCPDS 36-1451
1	15.8707	31.7415	100	0.2333	59.46nm	44±50	31.770
2	17.2002	34.4004	002	0.2645	52.42nm		34.422
3	18.1168	36.2337	101	0.2602	53.28nm		36.353
4	23.7669	47.5338	102	0.3207	43.23nm		47.539
5	28.2994	56.5988	110	0.3194	43.42nm		56.603
6	31.4360	62.8720	113	0.3751	36.97nm		62.864
7	33.1954	66.3909	200	0.3580	38.73nm		66.378
8	33.9862	67.9724	112	0.3876	35.77nm		67.961
9	34.5500	69.1000	201	0.4019	34.50nm		69.100

S2							Stand $2\theta(^{\circ})$ JCPDS 36-1451
No.	$\theta(^{\circ})$	$2\theta(^{\circ})$	Hkl	FWHM	Size	D(nm)	
1	15.8928	31.7856	100	0.2741	29.72nm	42±30	31.770
2	17.2220	34.4441	002	0.2598	17.13nm		34.422
3	18.1206	36.2412	101	0.3839	36.12nm		36.353
4	23.7905	47.5810	102	0.2939	54.80nm		47.539
5	28.3224	56.6449	110	0.3619	38.33nm		56.603
6	31.4572	62.9145	113	0.3468	41.63nm		62.864
7	33.2147	66.4295	200	0.3750	42.11nm		66.378
8	34.0056	68.0112	112	0.2280	73.24nm		67.961
9	34.5673	69.1346	201	0.3659	47.49nm		69.100

S3							Standard $2\theta(^{\circ})$ JCPDS 36-1451
No	$\theta(^{\circ})$	$2\theta(^{\circ})$	Hkl	FWHM	Size	D(nm)	
1	15.9074	31.8149	100	0.5686	14.20nm	30±32	31.770
2	17.1854	34.3708	002	0.2745	16.42nm		34.422
3	18.1024	36.2048	101	0.3557	33.82nm		36.353
4	23.7504	47.5008	102	0.4319	36.63nm		47.539
5	28.2855	56.5711	110	0.4149	32.77nm		56.603
6	31.4199	62.8398	113	0.4417	32.22nm		62.864
7	33.1822	66.3645	200	0.3790	40.74nm		66.378
8	33.9632	67.9264	112	0.4990	32.60nm		67.961
9	34.5205	69.0411	201	0.5064	33.49nm		69.100

The calculated particles sizes are in the range of nanoscale (1nm -100nm) and are applicable for textiles materials [21]. Table 4.1 also, shows that calculated “D” values are in good agreement with those taken from Joint Committee on Powder Diffraction Standard (JCPDS) card file data for ZnO nano powder i.e. the prepared materials have crystallized in a hexagonal wurtzite structure. The lattice parameter and the unit cell volume of synthesized ZnONPs were calculated by the equation (4.2), (4.3), (4.4) and recorded into table 4.2.

$$a = \sqrt{\frac{1}{3} \frac{\lambda}{\sin \theta}} \text{ and } c = \frac{\lambda}{\sin \theta} \quad (4.2)$$

$$d_{hkl} = \frac{ac}{2} \sqrt{\frac{3}{c^2(h^2+hk+k^2) + \frac{3(a)^2}{4}}} \quad (4.3)$$

$$V = \frac{\sqrt{3}}{2} a^2 c \quad (4.4)$$

Where d_{hkl} is spacing distance, a, b are lattice parameter, and V is volume cell [5, 10].

Table 4.2. Lattice parameters, unit cell volume, and c/a ratio of ZnONPs

Samples	hkl	Lattice parameter			d_{hkl} (nm)	Unit cell volume(nm)	JCPDS card number(36-1451)
		a(nm)	c(nm)	c/a (nm)			
S1	101	0.3504	0.5305	1.5135	0.2848	0.056	a=b=0.3249 c=0.5206
S2	101	0.3503	0.5604	1.5997	0.1869	0.059	
S3	101	0.2505	0.4608	1.839	0.2867	0.028	

All X-Ray diffraction peaks of synthesized ZnONPs using samples S1, S2, and S3, were shown slight agreement with wurtzite structure of ZnONPs with lattice parameter of $a = b = 0.3249$ nm and $c = 0.5206$ nm as reported in Joint Committee on Powder Diffraction Standard (JCPDS) card number 36-1451. The lattice parameter 'a', 'c' ' d_{hkl} ' and volume cell of ZnO NPs using samples S1, S2, and S3 for 101peak were calculated and small deviation in lattice parameter values were observed. The deviation may be caused due to slight change in the position of the peaks due to defect [22, 23].

3.2 SEM Analysis of ZnONPs

Figure 4.2 shows the SEM images of the synthesized ZnONPs using Samples S1, S2 and S3 at constant annealing temperature of 400°C. As it is shown below, the morphology of the particles are uniform and well dispersed flower shapes for synthesized ZnONPs using S1, spherical shape for synthesized ZnONPs using both S2, and S3. The SEM image results also agreed with XRD results obtained, i.e. the crystal sizes in XRD with large size have also large shapes in SEM images. This indicates that ZnONPs have successfully prepared using different zinc salt precursors within a nano range.

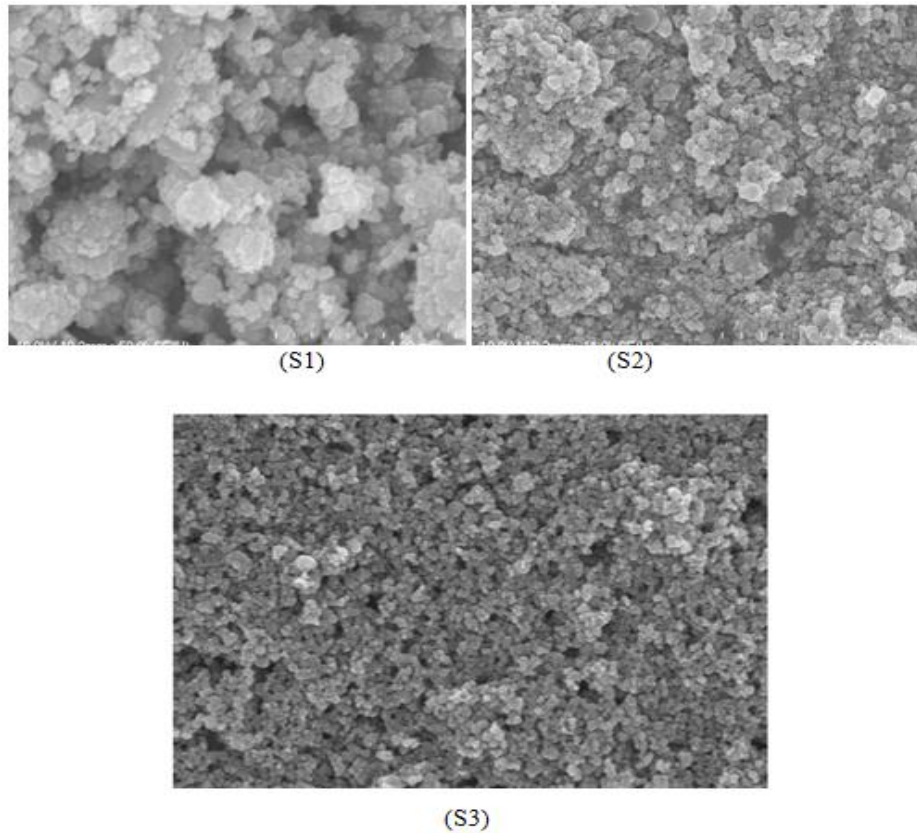


Figure 1.2 SEM images of synthesized ZnONPs from S1) PVA and $Zn(NO_3)_2 \cdot 6H_2O$, S2) NaOH and $Zn(CH_3COO)_2 \cdot 2H_2O$ and S3) NaOH and $ZnSO_4 \cdot 7H_2O$

3.3 UV/Visible Analysis of ZnONPs

Figure 4.3 shows UV/vis absorption spectra of synthesized ZnONPs using samples S2, S1, and S3 at constant annealing temperature of 400°C. The absorption peak was observed at 350nm and 390nm using sample S1, 378nm and 380nm using sample S2 and S3, respectively.

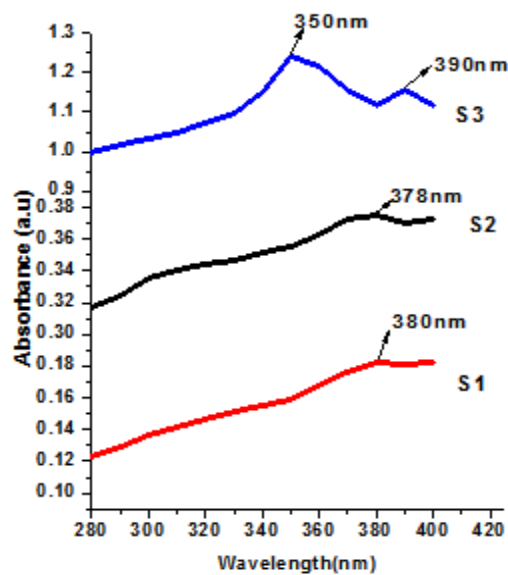


Figure 4.3 Absorption spectrum of synthesized ZnONPs using sample S1, S2, and S3

The band gap energy of synthesized samples were calculated by using the absorption edge relation of equation (4.5) below [24-27]

$$E_g = hv_g = \frac{hc}{\lambda_g} \quad (4.5)$$

Where $h = 4.14 \times 10^{-15} \text{ eVs}$, $C = 2.99 \times 10^8 \text{ m/s}$ and λ is wave length.

and exhibits 3.536eV, 3.274eV, and 3.257eV using sample S1, S2, and S3 respectively are good agreement with review literature. The energy band-gap of the ZnO nanoparticles was blue-shifted by the quantum confinement effect when compared with bulk ZnO. The peaks were due to electronic transition from valiancy band to conduction band.

3.4 Application of ZnONPs on Cotton Textiles

The application of nano sized ZnONPs on the cotton fabric increases the absorption of UV light. The performance of zinc oxide nanoparticles as UV absorbers was efficiently transferred to the fabric materials through the application of ZnO nanoparticles on the surface of the cotton fabrics. Figure 4.4 shows, absorbance spectra of cotton fabric in the range of 200nm-500nm. Higher values of UV absorbance were obtained when ZnONPs were synthesized from polyvinyl alcohol and zinc nitrate hex-hydrate (S1) is applied on cotton textiles. Higher absorbance of treated cotton textiles were observed at 376nm and 295nm which is in the range of UV-A and UV-B respectively while untreated cotton textile (S4 in figure 4.4) does not absorb UV-radiation.

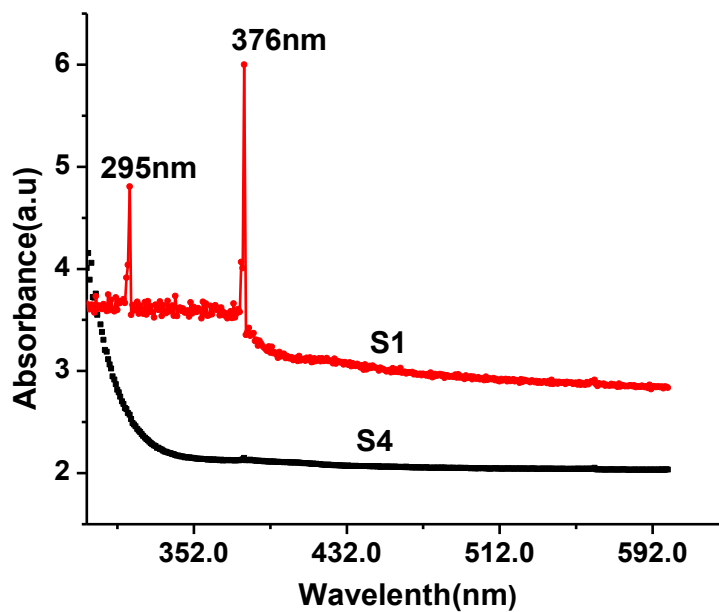


Figure 4.4: Absorption spectra of S4) Untreated cotton textile, S1) Treated cotton textiles by ZnONPs, synthesized from PVA and $Zn(NO_3)_2 \cdot 6H_2O$

Figure 4.5 shows, wavelength versus absorbance of treated and untreated cotton textiles synthesized from sodium hydroxide and zinc acetate (Sample S2). Higher UV absorbance was observed at 376nm and 300nm which is in the UV-A and UV-B respectively while untreated cotton was transparent i.e. untreated cotton textiles does not absorb UV-radiation.

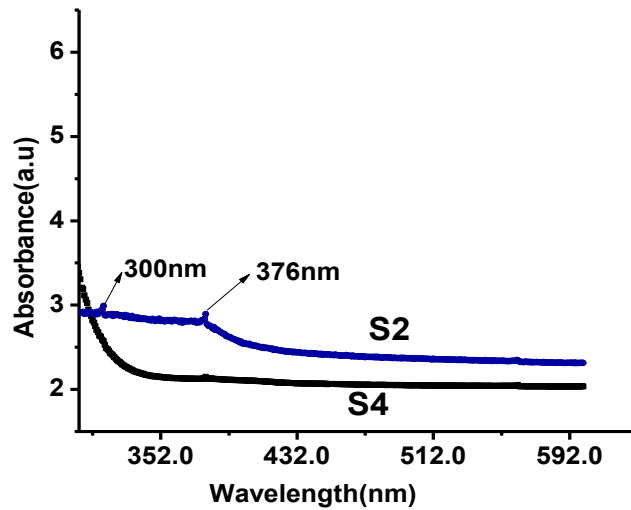


Figure 4.5. Absorption spectra of S4) Untreated cotton textile, S2) Treated cotton textiles by ZnONPs Synthesized from NaOH and Zn(CH3COO)2. 2H2O

Figure 4.6 shows, wavelength versus absorbance of treated and untreated cotton textiles synthesized from sodium hydroxide and zinc sulphite (Sample S3). Higher UV absorbance was observed at 290nm and 379nm which is in the range of UV-A and UV-B while untreated cotton does not absorb UV radiation.

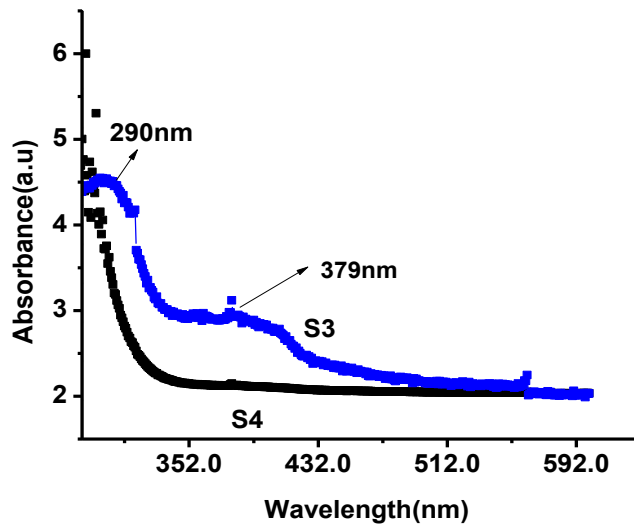


Figure 4.6. Absorption spectra of S4) untreated cotton textile, S3) Treated cotton textiles with ZnONPs synthesized from NaOH & ZnSO4.7H2O

The value of ultraviolet protection factor (UPF) and percent of transmittance (%T) were calculated according to the following equation (4.6) and (4.7) as shown in table 4.3.

$$UPF = \int_{\lambda_1}^{\lambda_2} \frac{E(\lambda).S(\lambda)}{E(\lambda).S(\lambda).T(\lambda)} d\lambda \tag{4.6}$$

$$\% \text{ Transmittion} = \sum_{\lambda_1}^{\lambda_2} \frac{T(\lambda)}{\lambda_2 - \lambda_1} \tag{4.7}$$

Where $E(\lambda)$ is the relative erythermal spectral effectiveness, $S(\lambda)$ is the solar spectral irradiance in $\text{Wm}^{-2}\text{nm}^{-1}$ and $T(\lambda)$ is the spectral transmission specimen obtained from UV spectrometric experiments, $E(\lambda)$ and $S(\lambda)$ were obtained from the national oceanic and atmospheric administration data base (NOAA) [18,29]. The application of nano sized ZnONPs on a cotton textiles increases UV light absorbance. The result implies that, the effectiveness in shielding UV radiation is due to the UV absorbance capacity of ZnONPs on the cotton textiles surface. The percent of transmittance confirm this conclusion as the ZnONPs treated cotton has low percent of transmittance while untreated fabrics has high percent of transmittance (table 4.3).

Table 3.3. UV-blocking properties of the cotton fabrics

Samples	Transmittance (%)	UPF	Protection Categories
S1	2.65	61.50	Excellent
S2	6.23	43.32	Very good
S3	7.83	39.34	Very good
S4	74.56	1.63	Pure

The spectrum of the cotton textiles showed that, high percent of transmittance in case of sample S4 has low UV-blocking ability i.e. untreated cotton textiles penetrate ultra violet radiation when compared to these treated cotton textiles results. Low percentage of transmittance spectrum of the cotton textiles S1 sample demonstrated increased UV-blocking ability, compared to the sample S2 and S3 results excellent protection categories.

IV. CONCLUSION

ZnONPs were synthesized via sol-gel method by using zinc nitrate hex-hydrate, zinc sulphate heptahydrate, and zinc acetate as a precursor with polyvinyl alcohol and sodium hydroxide. The synthesized ZnONPs were characterized by using different spectroscopic techniques such as XRD, SEM, and UV/vis spectroscopy. The XRD analysis revealed that the synthesized nanoparticles were in nanometer range with average particle size of 44.20nm, 42.30nm and 30.30nm using Debye Scherer's formula for samples S1, S2 and S3 respectively. The absorbance peak of synthesized ZnONPs using sample S1, S2, and S3 were investigated from UV/vis spectroscopy were 350nm, 378nm and 380nm respectively. The effect of optical properties of ZnONPs was investigated using UV/Vis spectroscopy. The morphology of ZnONPs were characterized by SEM shows flower and spherical shape. The SEM image results were agreed with XRD results i.e. the crystal sizes in XRD with large size have also large shapes in SEM images. The strong performance of ZnONPs as UV absorbers can be efficiently transferred to textiles materials through the application of ZnONPs on the surface of cotton textiles. The UV/Visible tests indicate that an increment of UV/absorbing activity of ZnO NPs treated cotton textiles. The absorption capacity of ZnONPs on the cotton textiles surface

gives effectiveness in shielding UV radiation. The calculated value of ultraviolet protection factor (UPF) and percent of transmittance (%T) were reflects the protection against UV radiation provided by the ZnO nanoparticles treated textiles. This result can be exploited for the protection of the body from the impact of UV-radiation.

Data availability

The data used to write this manuscript to support the findings of this study are included within the article.

Conflicts of interest

The authors declare that there is no conflict of interest regarding to publication of this paper.

Acknowledgments

The authors would like to acknowledge staff of Dambi Dollo University for their indefinite support during our paper writing, Adama Science and Technology University department of physics for allowing us the laboratory equipments/apparatus, Department of Material Science for allowing us XRD, SEM and finally, Addis Ababa University Department of Physics for allowing us UV/Visible Spectroscopy for characterizations of our samples.

REFERENCES

- [1]. S.A. Noorian, N. Hemmatinejad, J.A. Navarro Int. J. Bio. Macro., 154 (2020), pp. 1215-1226.
- [2]. N. A. Ibrahim, A.A. Nada, B.M. Eid, M. Al-Moghazy, A.G. Hassabo, N.Y. Abou-Zeid, Adv. Natar. Sci. Nanosci. Nanotechn., 9 (2018), p. 035014.
- [3]. A.A.M. Attia, M.S. Antonious, M.A.H. Shouman, A.A.A. Nada, K.M. Abas Carb. Lett., 29 (2019), pp. 145-154.
- [4]. S. Preethi, K. Abarna, M. Nithyasri, P. Kishore, K. Deepika, R. Ranjithkumar, V. Bhuvaneshwari, D. Bharathi Int. J. Biol. Macro., 164 (2020), pp. 2779-2787.
- [5]. B. Abebe, B. Bulcha, A.R. Chandra Reddy J. Nanotechn. Mat. Sci., 5 (2018), pp. 44-50.
- [6]. A.G. Hassabo, M.E. El-Naggar, A.L. Mohamed, A.A. Hebeish Carbohydr. Poly., 210 (2019), pp. 144-156.
- [7]. M.E. El-Naggar, S. Shaarawy, A .A. Hebeish, Carbohydr. Poly., 181 (2018), pp. 307-316.
- [8]. A. Fouda, E.L. Saad, S.S. Salem, T.I. Shaheen Microbial pathogen., 125 (2018), pp. 252-261.
- [9]. A.V. Abramova, V.O. Abramov, V.M. Bayazitov, Y. Voitov, E.A. Straumal, S.A. Lermontov, T.A. Cherdynitseva, P. Braeutigam, M. Weiße, K. Günther, Ultrason. Sonochem., 60 (2020), p. 104788.
- [10]. A. M. Holi, A. A. Al-Zahrani, A.S. Najm, P. Chelvanathan, N.Amin Chem. Phys. Lett., 89 (2020), p. 137486.

- [11]. E.Y.N.Yuen, T. Knight, S. Dodson, L. Ricciardelli, S. Burney P.M. Livingston, Baseboard Manag. Contr. Fam. Pract., 15 (2014), pp. 1-12.
- [12]. A. Verbic, M. Gorjanc, B. Simoncic Recent adv. Coatings, 9 (2019), p. 550.
- [13]. B.S. Butola, A. Kumar, Int. J. Biol. Macromol., 152 (2020), pp. 1135-1145.
- [14]. H.Y. Phin, Y.T. Ong, J.C. Sin, J. Env. Chem. Eng., 8 (2020), p. 103222.
- [15]. S. Mahmud, N. Pervez, M.A. Taher, K. Mohiuddin, H.H. Liu, Textile research journal, 90 (2020), pp. 1224-1236.
- [16]. M. Maghima, S. A. Alharbi J. Photochem. Photobiol. B Biol., 204 (2020), p. 111806.
- [17]. S. Chakrabarti, P. Banerjee J. Textile Institute, 106 (2015), pp. 963-969.
- [18]. M. Fiedot-Toboła, M. Ciesielska, I. Maliszewska, O. Rac-Rumijowska, P. Suchorska-Woźniak, H. Teterycz, M. Bryjak, Mater. Sci., 11 (2018) p. 707.
- [19]. T.R. Kar, A.K. Samanta, M. Sajid, and R. Kaware, Text. Resear. J., 89 (2019) pp. 2260-2278.
- [20]. G. Singh, E.M. Joyce, J. Beddow, T.J. Mason, J. microbial., biotechnol. food sci., 9 (2020), pp. 106-120.
- [21]. A. Yadav, V. Peasad, A.A. Kathe, S. Raj, D. Yadav, C. Sundaramoorthy, N. Vigneshwaran, Bulletin Mater. Sci., 29 (2006) pp. 641–645.
- [22]. R. Pandimurugan, S. Thambidurai, Intern. J. Biol. Macromol., 105 (2017), pp. 788-795.
- [23]. N.A. Ibrahim, A. A. Nada, A. G. Hassabo, B. M. Eid, A. M. Noor El-Deen, N. Y. Abou-Zeid, Chemic. Papers, 71 (2017), pp. 1365-75.
- [24]. J.A. Shirley, S.E. Florence, B.S. Sreeja, G. Padmalaya, S. Radha, J. Mater Sci. Mater.Electronics, 79 (2020), pp. 1-12.
- [25]. S.M. Costa, D.P. Ferreira, A. Ferreira, F. Vaz, R. Figueiro, Nanomater. 8 (2018), p. 1069.
- [26]. S.M. Sharaf, S.E. Talat, G.E. Salem, H.A. Hendawy, J. Microbiol., vol. 52 (2019), pp. 89.
- [27]. L.E. Román, J. Huachani, C. Uribe, J.L. Solís, M.M. Gómez, S. Costa, S. Costa, Appl. Surf. Sci., 469 (2019), pp.204-212.
- [28]. G.D. Patil, A.H. Patil, S.A. Jadhav, C.R. Patil, P.S. Patil Mater. Lett., 255 (2019), p. 126562.
- [29]. I. Boticas, D. Dias, D. Ferreira, P. Magalhães, R. Silva, R. Figueiro, SN Appl.Sci., 1 (2019), p.1376.
- [30]. J. Singh, S. Kumar, A.K. Manna, R.K. Sonny, Opt. Mater., 107 (2020), p.110138.